

# Local roughness exponent in the nonlinear molecular-beam-epitaxy universality class in one-dimension

Edwin E. Mozo Luis,<sup>1,\*</sup> Thiago A. de Assis,<sup>1,†</sup> Silvio C. Ferreira,<sup>2,3,‡</sup> and Roberto F. S. Andrade<sup>1,3,§</sup>

<sup>1</sup>*Instituto de Física, Universidade Federal da Bahia, Campus Universitário da Federação,  
Rua Barão de Jeremoabo s/n, 40170-115, Salvador, BA, Brazil*

<sup>2</sup>*Departamento de Física, Universidade Federal de Viçosa, Minas Gerais, 36570-900, Viçosa, Brazil*

<sup>3</sup>*National Institute of Science and Technology for Complex Systems, 22290-180, Rio de Janeiro, Brazil*

We report local roughness exponents,  $\alpha_{\text{loc}}$ , for three interface growth models in one dimension which are believed to belong the non-linear molecular-beam-epitaxy (nMBE) universality class represented by the Villain-Lais-Das Sarma (VLDS) stochastic equation. We applied an optimum detrended fluctuation analysis (ODFA) [Luis *et al.*, *Phys. Rev. E* **95**, 042801 (2017)] and compared the outcomes with standard detrending methods. We observe in all investigated models that ODFA outperforms the standard methods providing exponents in the narrow interval  $\alpha_{\text{loc}} \in [0.96, 0.98]$  consistent with renormalization group predictions for the VLDS equation. In particular, these exponent values are calculated for the Clarke-Vvedensky and Das Sarma-Tamborenea models characterized by very strong corrections to the scaling, for which large deviations of these values had been reported. Our results strongly support the absence of anomalous scaling in the nMBE universality class and the existence of corrections in the form  $\alpha_{\text{loc}} = 1 - \epsilon$  of the one-loop renormalization group analysis of the VLDS equation.

PACS numbers: 81.15.Aa, 05.40.-a, 68.35.Ct

## I. INTRODUCTION

Kinetic roughening is an important feature related to the growth of interfaces under nonequilibrium conditions [1, 2]. In many systems under specified conditions, including that of molecular-beam epitaxy (MBE) experiments, the surface diffusion may be a ruling mechanism competing with the deposition [1, 3]. Stochastic modeling of MBE is a frontline scientific issue since it corresponds to a technique to produce high quality thin films for many applications [3, 4]. In the simplest cases, the modeling assumes a limited mobility of adatoms. Some examples include the conservative restricted solid-on-solid (CRSOS) [5, 6] and the Das Sarma and Tamborenea (DT) [7] models, in which short-range surface diffusion and permanent aggregation take place after adsorption. More realistic models include thermally activated processes where the mobility is not limited. A noteworthy one is the Clarke-Vvedensky (CV) model [8–11], in which the adatom diffusion rates follow Arrhenius laws, with energy barriers depending on the local number of bonds. Recently, the scaling properties of a limited-mobility model were compared with the CV model [12], discussing the effects of memory (non-Markovianity) and probabilities of adatom detachment from terrace steps. It was observed that many central features of thermally activated models can be captured with their limited mobility versions [12].

The CRSOS [13], DT [7, 14] and CV [8, 9, 11] models are connected with the nonlinear molecular-beam-epitaxy (nMBE) universality class, since the surface dynamic is ruled by adatom diffusion. If the incoming particle flux is omitted, the corresponding nMBE growth equation, also called Villain-Lai-Das Sarma (VLDS) [15, 16], is given by

$$\frac{\partial h}{\partial t} = -\nu_4 \nabla^4 h + \lambda_4 \nabla^2 (\nabla h)^2 + \eta(\mathbf{x}, t), \quad (1)$$

where  $h$  corresponds to the height, at the position  $\mathbf{x}$  and time  $t$ , with respect to the initial  $d$ -dimensional substrate,  $\nu_4$  and  $\lambda_4$  are constants and  $\eta(\mathbf{x}, t)$  is a nonconservative Gaussian noise.

In this work, we investigate interface growth on one-dimensional substrates. The growth ( $\beta$ ) and the dynamical ( $z$ ) exponents are used as benchmarks to describe the interface scale invariance [1]. The former exponent characterizes how height fluctuations  $\omega$  while the latter how the characteristic correlation length  $\xi$  evolve, usually obeying scaling laws of the forms  $\omega \sim t^\beta$  and  $\xi \sim t^{1/z}$ , respectively. The global roughness exponent  $\alpha = \beta z$  can also be used in the regime where the correlation length is much larger than the scale of observation  $L$  when  $\omega \sim L^\alpha$  [1, 17]. According to a dynamical one-loop renormalization-group (RG) analysis of Eq. (1), the roughness and dynamic exponents are given by  $\alpha = (4 - d)/3$  and  $z = (8 + d)/3$ . However, Janssen [18] pointed out that this conclusion was derived from an ill-defined transformation and there would be higher order corrections. For instance, small negative corrections to  $\alpha$  and  $z$  were reported in all dimensions from a two-loop calculation [18]. These corrections are supported by numerical results for CRSOS model [19], in which  $\alpha = 0.94(2) < 1$ , the predicted value by the

\* eluis@ufba.br

† thiagoaa@ufba.br

‡ silviojr@ufv.br

§ randrade@ufba.br

one-loop RG analysis  $\alpha = 1$ .

Nonetheless, several investigations of nMBE lattice models formerly suggested that the local and global height fluctuations scale with different local and global roughness exponents, characterizing an anomalous scaling [20, 21]. To define this phenomenon, let us consider the interface fluctuations within a window of length  $r$  and at time  $t$  (hereafter called quadratic local roughness)

$$\omega_i^2(r, t) = \langle h^2 \rangle_i - \langle h \rangle_i^2, \quad (2)$$

where  $\langle \dots \rangle_i$  means averages over the window  $i$ . The quadratic local interface roughness  $\omega^2(r, t)$  is defined considering the average of  $\omega_i^2$  over different windows and independent realizations. In normal dynamical scaling, in which the Family-Vicsek ansatz [17] holds, the local roughness for a window of length  $r$  increases as  $\omega \sim t^\beta$  for  $t \ll r^z$  and saturates as  $\omega \sim r^{\alpha_{\text{loc}}}$  for  $t \gg r^z$ , with  $z = \alpha_{\text{loc}}/\beta$ . The exponent  $\alpha_{\text{loc}}$  is the local roughness or Hurst exponent [1]. Anomalous scaling happens when local and global roughness exponents are different implying that the local roughness presents dependence on both window size and time at short scales given by  $\omega(r, t) \sim r^{\alpha_{\text{loc}}} t^\kappa$  with  $\kappa = (\alpha - \alpha_{\text{loc}})/z$ .

Anomalous scaling was reported in theoretical analyzes of epitaxial surface growth and numerical integration of the VLDS equation in  $d = 1$  and 2 [22]. Mound formation was claimed to justify the anomalous scaling, which contrasts with the conclusions reported in Refs. [20, 23], according to which normal scaling should occur in local growth processes. Crystalline mounds have been also used to justify anomalous scaling in experiments [24], while the interplay between nonlocal strain and substrate disorder was pointed out as a mechanism involved in the anomalous scaling in epitaxial growth of semiconductor CdTe films [25, 26].

In the context of lattice models, it was reported an apparent anomalous scaling at short times which asymptotically turns into normal scaling for the CRSOS model [23]. The local roughness exponent of the DT model was reported to be  $\alpha_{\text{loc}} \approx 0.7$  in  $d = 1$  [27, 28]. This value is different from the global roughness exponent  $\alpha = 1 - \epsilon$  predicted in the RG analysis of the VLDS equation, which might suggest anomalous roughening [29, 30]. However, the local roughness distributions [23] suggest that the one-dimensional DT model has normal scaling, in agreement with the predictions of dynamic RG analysis for local growth process without quenched disorder or additional symmetries [20]. Thus, the DT model remains controversial and a careful consideration regarding their local roughness exponents, especially without noise reduction techniques [31–33], is worthwhile.

An evaluation of  $\alpha_{\text{loc}}$  for CV model in two-dimensions, in agreement with the nMBE class, was recently reported [34]. The effective roughness exponent was calculated with the optimal detrended fluctuation analysis (ODFA), while the exponents obtained with other methods did not match with those of the nMBE class [34]. This result provided support for non-anomalous asymptotic

scaling in CV model, corroborating the claim that this transient effect is a consequence of large corrections to the asymptotic normal scaling [11]. However, an explicit observation of the local roughness exponent for the CV model in  $d = 1$  is still missing.

Motivated by the aforementioned studies, we present an analysis of the local roughness exponent for CRSOS, DT and CV models in one-dimension using the ODFA method. Our results show that the second order ODFA method suitably yields values of  $\alpha_{\text{loc}}$  consistent with the nMBE class for CRSOS and CV models. Moreover, the obtained exponents corroborate the existence of corrections in the one-loop RG [18]. For DT models, the ODFA method also provides values in agreement with nMBE class specially in the case of mild noise reductions [31–33]. In the original DT, two scaling regimes were observed: at short scales we report  $\alpha_{\text{loc}}^{(\text{DT})} \approx 0.90$  and at intermediary ones  $\alpha_{\text{loc}}^{(\text{DT})} \approx 0.97$ , both considerably closer to the nMBE class than the values found with other methods. The results presented here are consistent with the conjecture of Ref. [20], which argues that intrinsic anomalous roughening cannot occur in local growth models.

The rest of this paper is organized as follows. In section II, we present the models and basic concepts involved in this work. In section III, we discuss the limits where the ODFA method outperforms other methods, considering mounded initial conditions. In section IV, the scaling of surface roughness is analyzed and the local roughness exponent is reported. In section V, we summarize our conclusions and prospects.

## II. MODELS AND BASIC CONCEPTS

The lattice models studied in this work are the CRSOS, DT and CV. All simulations were performed on a initially flat one-dimensional substrate with  $L$  sites and periodic boundary conditions. One time unit corresponds to the deposition of  $L$  adatoms. In all models, deposition occurs with rate  $F = 1$  in a flux normal to the substrate and obeys a solid-on-solid condition [1].

In the CRSOS model, a site is randomly chosen for one adatom deposition. The height differences  $\delta h$  between nearest-neighbors obey the restriction  $\delta h \leq \delta H_{\text{max}}$ . We consider the case  $\delta H_{\text{max}} = 1$ . If this condition is satisfied for the randomly chosen incidence site, the particle permanently sticks there. Otherwise, it searches the nearest position where the condition is satisfied, which becomes the place of deposition. In the case of multiple options, one of them is randomly chosen.

In the CV model, deposition occurs at a constant and uniform rate while the adatom diffusion rate is given by an Arrhenius law in the form  $D = \nu_0 \exp(-E/k_B T)$  where  $\nu_0$  is an attempt frequency,  $k_B$  the Boltzmann constant, and  $E$  is an energy barrier for the hopping, which includes the contribution of the substrate ( $E_S$ ) and lateral bonds ( $E_N$ ) assuming the form  $E = E_S + nE_N$ . The ratio  $R = D_0/F$ , in which  $D = D_0 \epsilon^n$  is the hopping rate

if an adatom has  $n$  lateral neighbors, is a control parameter of the model [11, 34]. In this work we use  $R = 10$  and  $\varepsilon = 0.01$ , which leads to a large surface roughness, since it corresponds to a low temperature (low mobility) regime.

In the one-dimensional DT model [7], the arriving particle sticks at the top of the incidence site if there is one or two lateral bonds. Otherwise, if one of the nearest-neighbors satisfies this condition, it is chosen for the deposition whereas if both do, one of them is randomly chosen. If neither the deposition site nor any of the nearest-neighbors have lateral bonds, the particle sticks at the top of the incidence site. We also applied the noise reduction technique [32], in which a site must be selected  $M$  times before implementing a deposition. We considered the case of mild noise reduction  $M = 4$  where the interface roughness remains large.

A characteristic lateral surface length can be estimated as the first zero ( $\xi_0$ ) of the height-height correlation function defined as [3, 35, 36]

$$\Gamma(s, t) \equiv \left\langle \tilde{h}(s_0 + s, t) \tilde{h}(s_0, t) \right\rangle, \quad (3)$$

where  $\tilde{h} \equiv h - \bar{h}$ , and the averages are taken over different initial positions  $s_0$  and different configurations. The correlation length  $\xi_0$  is defined as the position of the first zero of the correlation function, i.e.  $\Gamma(\xi_0, t) = 0$  and are expected to scale as  $\xi_0(t) \sim t^{1/z_c}$ , where  $z_c$  is the coarsening exponent that usually corresponds to the dynamical exponent defined previously.

Figure 1 shows profiles for CRSOS, CV and DT models for times  $t = 10^6$  (CRSOS and CV) and  $t = 10^8$  (DT). One can see the presence of a characteristic length (mounded structures) for the CV and DT cases and a self-affine structure with less evident mounds for CRSOS model. As illustrated by the corresponding insets in Fig. 1, the estimated characteristic lengths  $\xi_0$  for CRSOS and CV correspond to  $\xi_0 \approx 433$  and  $\xi_0 \approx 74$ , respectively. For DT, the estimated values without and with noise reduction are  $\xi_0 \approx 299$  and  $\xi_0 = 564$ , respectively. Here, it is possible to note a decrease of the global roughness as  $M$  increases suppressing large hills and valleys in the surfaces. Concomitantly, an increase of the characteristic mound sizes is observed, which is reflected by an increasing of the correlation length.

### III. OPTIMAL DETRENDED FLUCTUATION METHOD

Let us start with the standard DFA method using a  $n$ th order polynomial to detrend the surface [37], called hereafter of  $\text{DFA}_n$ . The interface fluctuation within a window  $i$  of size  $r$  in  $\text{DFA}_n$  is defined as

$$\omega_i^{(n)} = \langle (\delta^{(n)})^2 \rangle_i^{1/2} \quad (4)$$

where

$$\delta^{(n)} = h(x) - G_i(x; A_i^{(0)}, A_i^{(1)}, \dots, A_i^{(n)}), \quad (5)$$

$G_i$  is a  $n$ th order polynomial regression of the interface within the  $i$ th window with coefficients  $A_i^{(0)}, A_i^{(1)}, \dots, A_i^{(n)}$  obtained using least-square method [38]. The local roughness yielded by the  $\text{DFA}_n$  method  $\omega^{(n)}$  is given by the average over different windows and samples. In the standard local roughness analysis, that corresponds to  $\text{DFA}_0$ , the surfaces fluctuations are computed in relation to the average height such that  $G_i = A_i^{(0)} = \langle h \rangle_i$ .

In the ODFA method, the local roughness in the window  $i$  of size  $r$  is defined by Eq. (4) with

$$\delta^{(n)} = \min_x \left[ h(x) - G_i(x; A_i^{(0)}, A_i^{(1)}, \dots, A_i^{(n)}) \right], \quad (6)$$

where  $\min_x$  represents minimal distance from the surface point with height  $h(x)$  to the polynomial  $G_i$ .

Differences between the exponents yielded by DFA and ODFA methods were reported [34] in the kinetic roughening obtained for the deposition on initially mounded substrates. The second order ODFA<sub>2</sub> method allows to capture the expected universality class of the fluctuations at scales shorter than the average mound length, whereas DFA<sub>2</sub> underestimates the exponents [34]. In both cases, the main advantage of the second order methods with respect to the first order ones are more extended regions of scaling, represented by longer plateaus in the effective roughness exponent,

$$\alpha_{\text{eff}} \equiv \frac{d [\ln \omega^{(n)}]}{d [\ln r]}, \quad (7)$$

as function of the scale  $r$ .

### IV. SCALING OF THE LOCAL SURFACE ROUGHNESS

Figure 2 shows the local roughness  $\omega^{(n)}$  as a function of the window size  $r$  for CRSOS, CV and DT models. The analyses using  $\text{DFA}_0$  indicate a local slope close to 0.7 at small scales ( $r \lesssim 10^2$ ) for all cases corroborating previous reports for models in the VLDS universality class [27, 28]. However, the slopes are close to  $\alpha_{\text{loc}} = 1$ , predicted by the one-looping RG approach [18], when we consider the scaling obtained from ODFA<sub>2</sub>.

In the case of the CRSOS model, DFA<sub>2</sub> and ODFA<sub>2</sub> methods provide very similar curves, confirmed in the local roughness exponent analysis of Figs. 2(a) and Fig. 3(a). This can be justified by the self-affine (fractal) geometry exhibited by the profile, as observed in Fig. 1(a), which implies in negligible differences between the height fluctuations determined either by Eq. (5) or (6). This fact is illustrated in Fig. 4(a), in which a zoomed part of a CRSOS profile is shown with the respective differences  $\delta_{\text{DFA}}^{(2)}$  and  $\delta_{\text{ODFA}}^{(2)}$  for some selected points. We also verified that the corresponding scaling of the second order methods are improved (the plateau region of the effective exponent analysis is larger) if compared

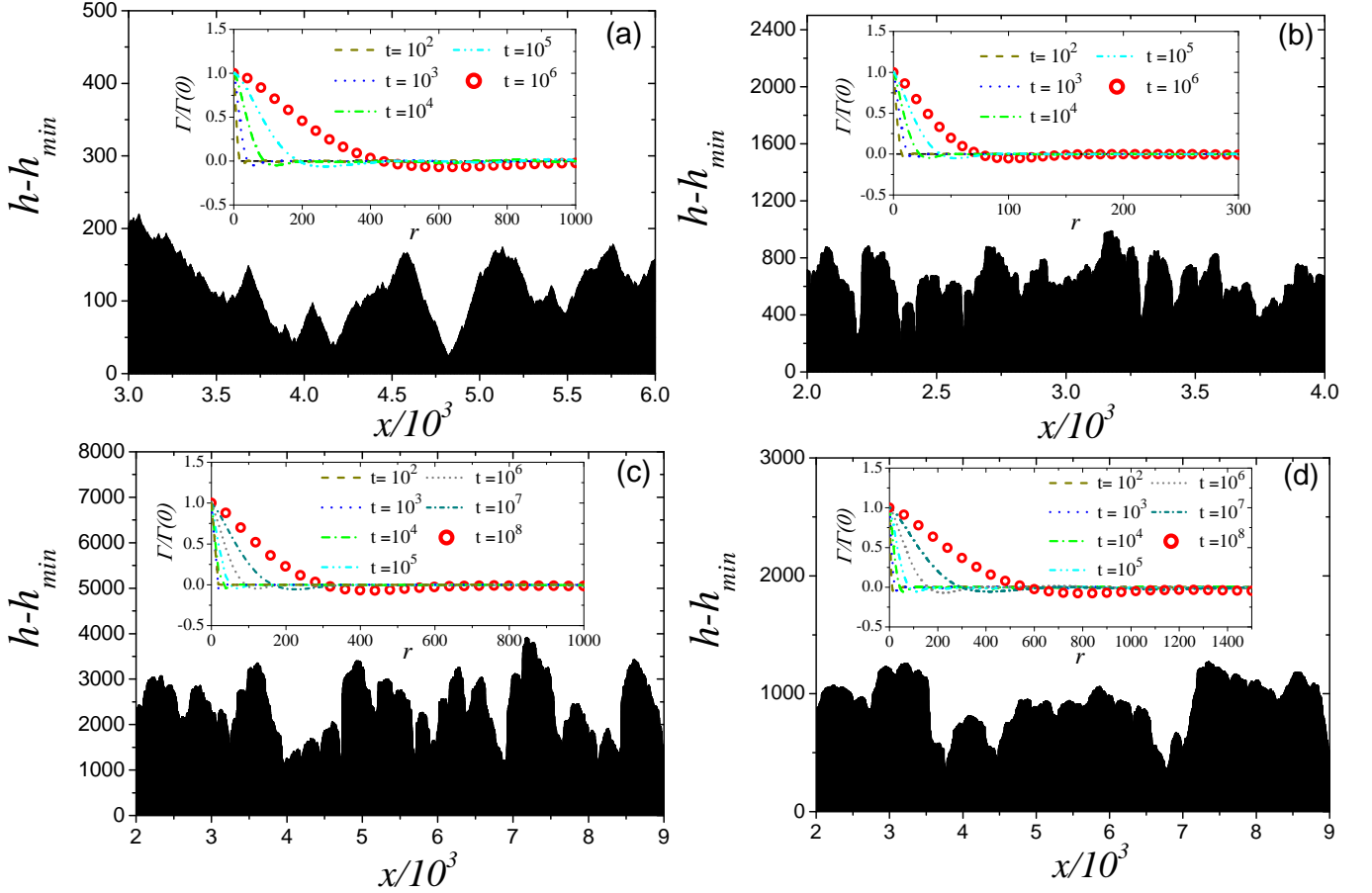


FIG. 1. Profiles for (a) CRSOS, (b) CV, and (c,d) DT models at  $t = 10^6$  (CRSOS and CV) and  $t = 10^8$  (DT). The simulations were performed on systems of size  $L = 2^{14}$ , assuring that the dynamics is not in the stationary regime of roughness saturation for the analyzed times. Insets show the corresponding normalized correlation function at different times, averaged over  $10^3$  independent realizations. Analysis for the DT model using noise reduction with  $M = 4$  is shown in (d).

with their first order counterpart, but the exponent values are approximately the same (results not shown). We determined the local roughness exponent of the CRSOS model in the plateau  $260 \lesssim r \lesssim 460$  shown in Fig. 3(a) and found  $\alpha_{\text{loc}}^{(\text{CRSOS})} = 0.983(1)$ , which is consistent with the claim of corrections in the one-loop RG analysis such that  $\alpha_{\text{loc}} = 1 - \epsilon$  [18]. Our result suggests that the corrections in the one-loop RG exponent are consistent with but not equal to that reported in two-loop RG calculations [18], as previously indicated elsewhere [19] for low dimensions. We stress that our result for  $\alpha_{\text{loc}}$  obtained for the CRSOS model, in which weak corrections to the scaling are expected, is slightly above (4% of deviation) to the global roughness exponent  $\alpha = 0.94(2)$  reported in Ref. [19], corroborating that the asymptotic anomalous scaling does not occur for this model.

Differences between ODFA<sub>2</sub> and DFA<sub>2</sub> methods are more evident for CV model as can be seen in Figs. 2(b) and 3(b). Again, the plateau is larger considering ODFA<sub>2</sub> as compared with ODFA<sub>1</sub> (data not shown). However, for ODFA<sub>1</sub> we obtained an effective roughness exponent  $\alpha_{\text{loc}}^{(\text{CV})} \approx 1.14(4)$  slightly larger than unity at

small scales, a spurious value that can be explained as a consequence of the large local slope in approximately columnar parts of the profile, as shown in Fig. 1(b). Indeed, the linear regression does not fit well the corresponding structures at small scales while the quadratic one does. Using the range  $50 \lesssim r \lesssim 170$ , which corresponds to the plateau shown in Fig. 3(b), the exponent obtained with ODFA<sub>2</sub> is  $\alpha_{\text{loc}}^{(\text{CV})} = 0.96(1)$ , in consonance with the normal scaling of the CV model observed in two dimensions [11, 34].

Figure 2(c) shows the local interface roughness for the DT model without noise reduction, in which noticeable differences can be seen in ODFA<sub>2</sub> and DFA<sub>2</sub> methods. One can see in Fig. 4(b) that the differences between the distances to the detrending curve using ODFA and DFA methods can be very large. A crossover between two scaling regimes is observed. For scales smaller than the characteristic length ( $0.23 \lesssim r/\xi_0 \lesssim 0.90$ ), a plateau is observed for ODFA<sub>2</sub> case, where the local roughness exponent was estimated as  $\alpha_{\text{loc}}^{(\text{DT})} = 0.903(1)$ , consistent with those found in the case of high noise reduction  $M \geq 64$  [32]. At larger scales ( $2.00 \lesssim r/\xi_0 \lesssim 2.51$ ),

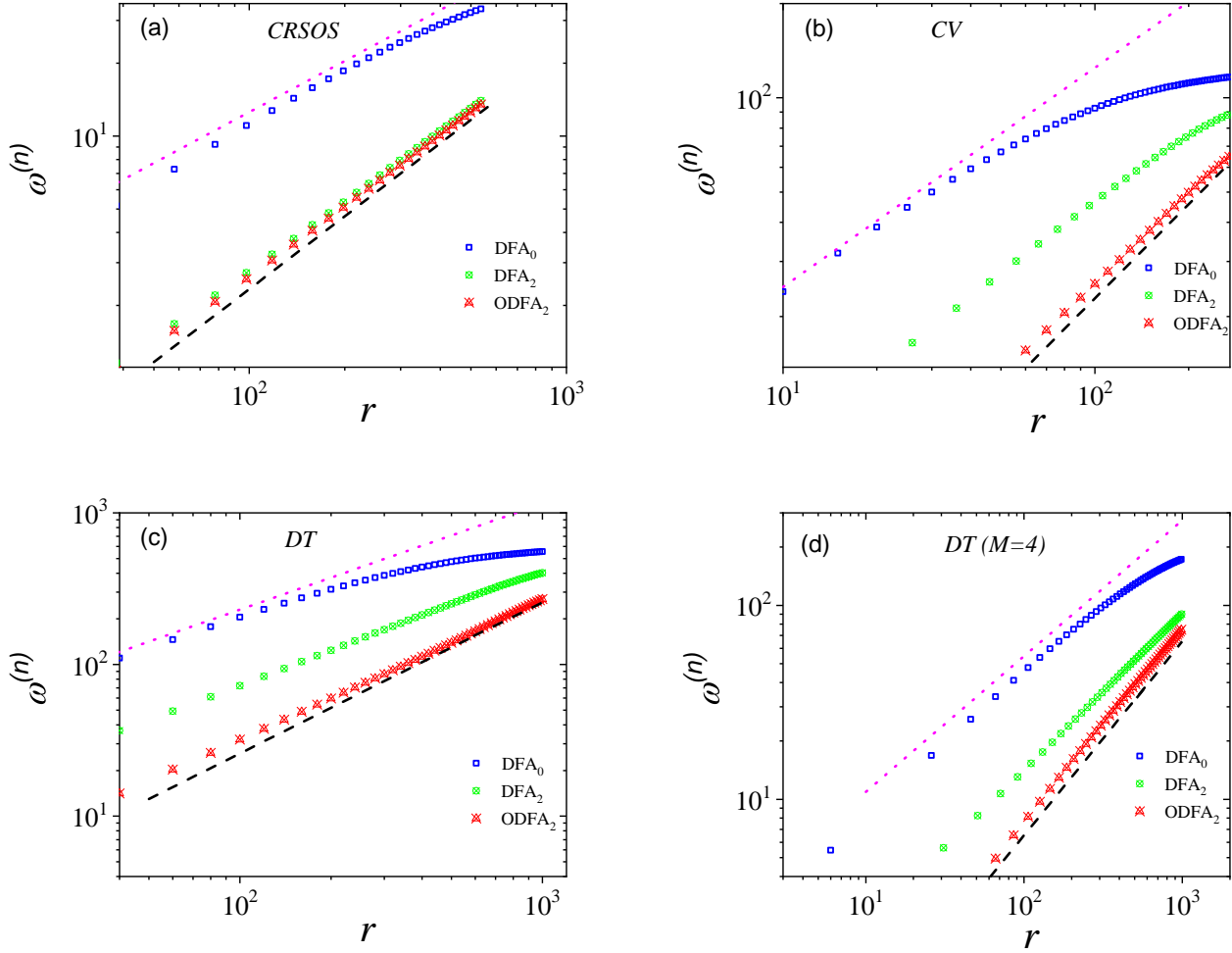


FIG. 2. Local roughness as a function of the window size using different methods for (a) CRSOS model at  $t=10^6$ ; (b) CV model at  $t=10^6$  and (c) DT model at  $t=10^8$ . The dotted and dashed lines have slopes 0.7 and 1, respectively. Averages were performed over up to  $10^3$  independent realizations. The system size is  $L=2^{14}$ . (d) The same analysis for the DT model using noise reduction with  $M=4$  [32].

$\alpha_{\text{loc}}^{(\text{DT})} = 0.976(1)$  was observed. To the best of our knowledge, ODFA<sub>2</sub> method for DT model yields a first evidence, without noise reduction techniques [31–33], of a roughness exponent consistent with the nMBE class (see Fig. 3(c)). Even though noise reduction should not change the universality class [39], very high levels reduce a lot the interface roughness, which becomes smoothed with a trending to provide an exponent close to 1. So, we have also analyzed the DT model with a mild noise reduction ( $M=4$ ). The interface roughness is reduced with respect to the original model but is still quite large, as can be seen in Fig. 4(c). The local roughness analyses are shown in Figs 2(d) and 3(d). With ODFA<sub>2</sub> we observed  $\alpha_{\text{loc}}^{(\text{DT})} = 0.967(2)$ , which is much closer to VLDS class than the value  $\alpha_{\text{loc}}^{(\text{DT})} = 0.804(7)$  obtained with DFA<sub>2</sub>. The latter is in good agreement with the  $\alpha_{\text{loc}}$  exponent reported in Ref. [32] for a similar noise reduction parameter. This result could lead to a misinterpretation

supporting anomalous scaling in DT model, since a large global roughness exponent  $\alpha \approx 1.2$  was also reported in Ref. [32] for this same range of  $M$ . Our results with ODFA<sub>2</sub> strongly suggest the absence of the anomalous scaling for the DT model too.

## V. CONCLUSIONS

The scaling properties of one-dimensional interfaces obtained with simulations of lattice models belonging to nMBE universality class is an issue that has attracted considerably attention [12, 13, 28, 32–35], given the outstanding importance of diffusion for applications in thin film growth [3, 4]. Differently from the Kardar-Parisi-Zhang [40] universality class that have a plenty of lattices models described by its scaling exponents [1, 2],



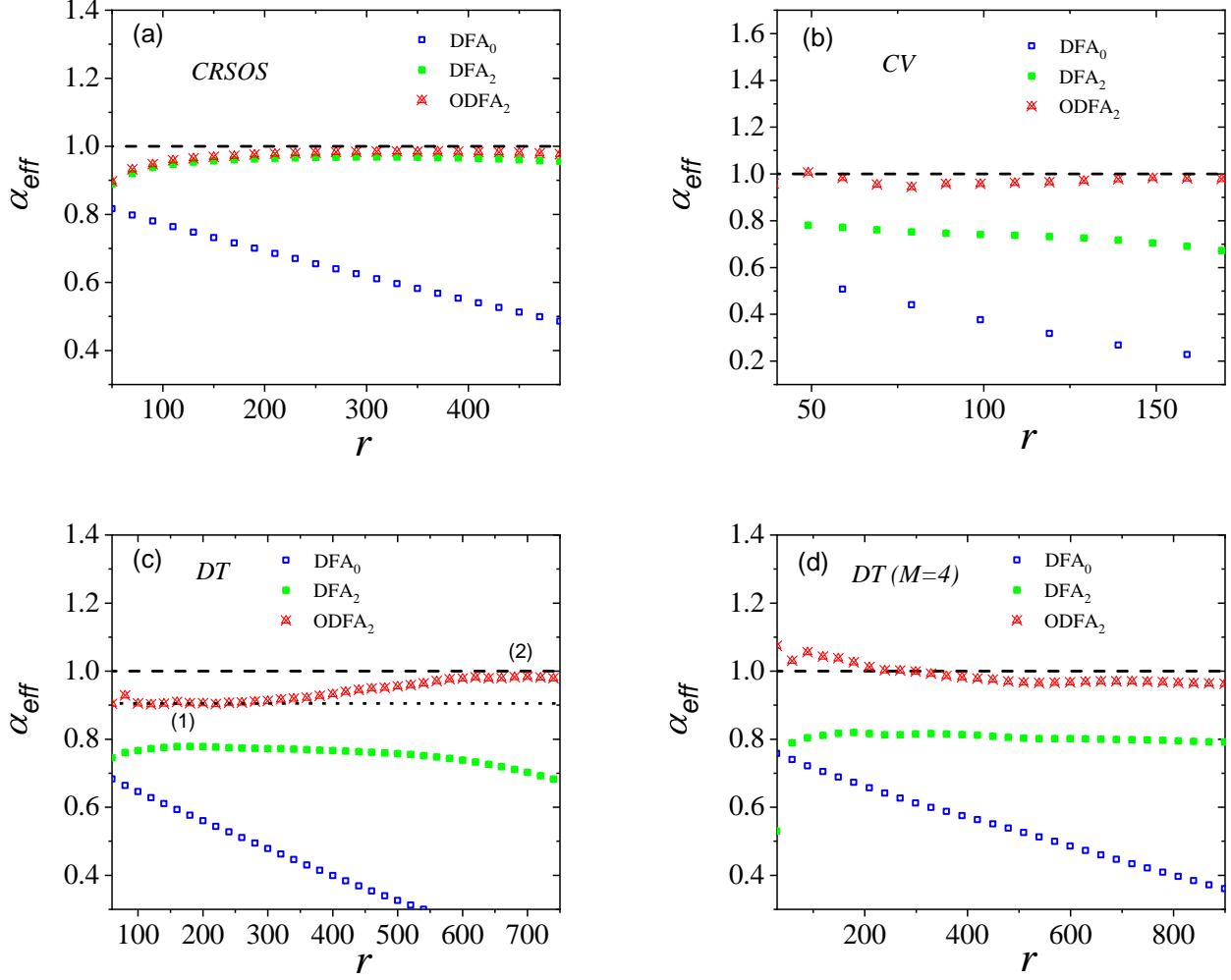


FIG. 3. Effective local roughness exponent analysis with different methods for (a) CRSOS model at  $t=10^6$ ; (b) CV model at  $t=10^6$  and (c) DT model at  $t=10^8$ . Two scaling regions are observed in the DT model at shorter and larger scales indicated by (1) and (2). The horizontal dashed lines indicate the value of the nMBE roughness exponent predicted by one-looping RG in  $d=1$  and the dotted line in (c) indicates the value 0.90. (d) The same analysis for the DT model using noise reduction with  $M=4$  [32].

the nMBE class, where diffusion is the ruling mechanism on the surface growth, has only a few basic prototypes. Three basic examples are the CRSOS [5, 6], CV [8, 9] and DT [7] models, which are investigated in the present work. To date, only the first one has been supported with irrefutable evidences that it belongs to the nMBE class. In the present work, we provide numerical analysis of the local roughness (Hurst) exponent [1, 37] of interfaces generated with these models, using the recently proposed optimal detrended fluctuation analysis [34], that is devised to investigate universality class in mounded structures. As in the two-dimensional analysis of mounded surfaces, the ODFA method [34] outperforms the standard DFA in the determination of the local roughness exponent  $\alpha_{\text{loc}}$ , as can be seen in table I, where a summary of the results reported in this paper is presented. For all investi-

gated models, the roughness exponent were found within the interval  $[0.96, 0.98]$ . This rules out the existence of asymptotic anomalous roughening sometimes claimed for these models [22] since these values are consistent with the predictions of the two-loop renormalization group developed by Janssen [18], where corrections in one-loop calculations of the form  $\alpha_{\text{loc}}^{(\text{VLDS})} = 1 - \epsilon$  are expected in all dimensions. To the best of our knowledge, this is the first evidence for the local roughness exponent measured in the DT model that agrees with the nMBE class. The original DT model still possesses a small ambiguity in the value of  $\alpha_{\text{loc}}$ : at short scales, the value  $\alpha_{\text{loc}}^{(\text{DT})} = 0.903$  is close to the VLDS exponent  $\alpha_{\text{loc}}^{(\text{VLDS})} = 1 - \epsilon$ , albeit still not negligibly below the VLDS value observed for intermediary scales, as shown in table I. However, a mild noise reduction is sufficient to remove very strong correc-

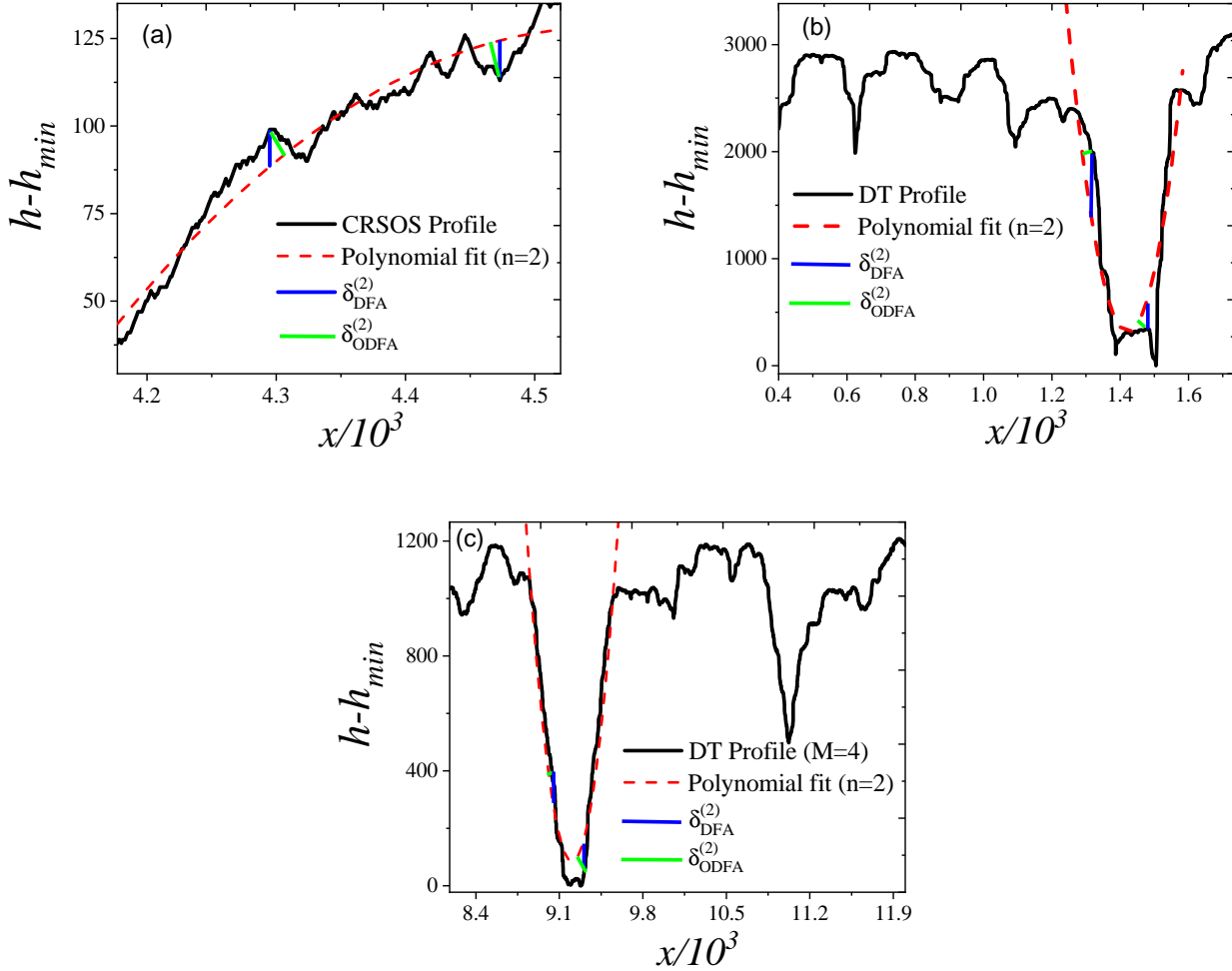


FIG. 4. Sections of the profiles shown with the second order polynomial regressions (dashed lines) for (a) CRSOS and (b)-(c) DT models. DT model is analyzed (b) without and (c) with noise reduction using  $M = 4$ . Selected points of the profile illustrates the differences between the  $\delta^{(2)}$  calculated with DFA and ODFA methods.

tions to the scaling and an accordance with the nMBE exponent is also found.

TABLE I. Values of the local roughness exponent calculated using the ODFA<sub>2</sub> and DFA<sub>2</sub> methods in the corresponding range of the ratio  $r/\xi_0$  (see also Fig. 3 for plateaus in the effective exponent analysis). The symbol \* means the absence of reliable scaling regimes in the corresponding range of  $r/\xi_0$ .

Model	$r/\xi_0$	ODFA <sub>2</sub>	DFA <sub>2</sub>
CRSOS	[0.6, 1.06]	0.983(1)	0.966(2)
CV	[0.67, 2.3]	0.96(1)	0.73(3)
DT [Region (1)]	[0.23, 0.90]	0.903(1)	0.772(6)
DT [Region (2)]	[2.00, 2.51]	0.976(1)	*
DT [ $M = 4$ ]	[0.88, 1.58]	0.967(2)	0.804(7)

Our findings constitute an important step for confirm-

ing the nMBE as a general universality class. Moreover, the scarcity of experimental evidences for nMBE could be explained by the almost unavoidable presence of strong corrections to the scaling due to limitations for growth times and resolution in scanning probe microscopes [41, 42], which might be addressed using suitable methods such as ODFA [34]. This method can be easily extended to the analysis of self-affine objects not related to surface growth such as time series modulated for seasonal changes [43]. Further enhancement of this method may include adapting it for global detrending which will allow the characterization of other features in interface growth such as properties of the underlying fluctuations in height distributions [44–46].

## ACKNOWLEDGMENTS

TAdA, SCF and RFSA thank the financial support of Conselho Nacional de Desenvolvimento Científico e

Tecnológico (CNPq). SCF acknowledges the support of Fundação de Pesquisa do Estado de Minas Gerais (FAPEMIG). This study was financed in part by the Coordenação de Aperfeiçoamento de Pessoal de Nível Superior - Brasil (CAPES) - Finance Code 001.

- 
- [1] A.-L. Barabasi and H. E. Stanley, *Fractal Concepts in Surface Growth* (Cambridge University Press, Cambridge, 1995).
  - [2] J. Krug, "Origins of scale invariance in growth processes," *Adv. Phys.* **46**, 139 (1997).
  - [3] J. Evans, P. Thiel, and M. Bartelt, "Morphological evolution during epitaxial thin film growth: Formation of 2D islands and 3D mounds," *Surf. Sci. Rep.* **61**, 1 (2006).
  - [4] M. Ohring, *Materials Science of Thin Films*, 2nd ed. (Academic Press, San Diego, USA, 2002).
  - [5] Y. Kim, D. K. Park, and J. M. Kim, "Conserved growth in a restricted solid-on-solid model," *J. Phys. A: Math. Gen.* **27**, L533 (1994).
  - [6] Y. Kim and J.-M. Kim, "Surface morphology, hopping, and current in a conserved growth model with a restricted solid-on-solid condition," *Phys. Rev. E* **55**, 3977 (1997).
  - [7] S. Das Sarma and P. Tamborenea, "A new universality class for kinetic growth: One-dimensional molecular-beam epitaxy," *Phys. Rev. Lett.* **66**, 325 (1991).
  - [8] S. Clarke and D. D. Vvedensky, "Origin of Reflection High-Energy Electron-Diffraction Intensity Oscillations during Molecular-Beam Epitaxy: A Computational Modeling Approach," *Phys. Rev. Lett.* **58**, 2235 (1987).
  - [9] S. Clarke and D. D. Vvedensky, "Growth kinetics and step density in reflection high-energy electron diffraction during molecular-beam epitaxy," *J. Appl. Phys.* **63**, 2272 (1988).
  - [10] M. Kotrla and P. Šmilauer, "Nonuniversality in models of epitaxial growth," *Phys. Rev. B* **53**, 13777 (1996).
  - [11] T. A. de Assis and F. D. A. Aarão Reis, "Dynamic scaling and temperature effects in thin film roughening," *J. Stat. Mech. Theory Exp.* **2015**, P06023 (2015).
  - [12] T. B. To, V. B. de Sousa, and F. D. Aarão Reis, "Thin film growth models with long surface diffusion lengths," *Physica A: Stat. Mech. Appl.* **511**, 240 (2018).
  - [13] S.-C. Park, D. Kim, and J.-M. Kim, "Derivation of continuum stochastic equations for discrete growth models," *Phys. Rev. E* **65**, 015102 (2001).
  - [14] M. Predota and M. Kotrla, "Stochastic equations for simple discrete models of epitaxial growth," *Phys. Rev. E* **54**, 3933 (1996).
  - [15] J. Villain, "Continuum models of crystal growth from atomic beams with and without desorption," *J. Phys. I* **1**, 19 (1991).
  - [16] Z.-W. Lai and S. Das Sarma, "Kinetic growth with surface relaxation: Continuum versus atomistic models," *Phys. Rev. Lett.* **66**, 2348 (1991).
  - [17] F. Family and T. Vicsek, "Scaling of the active zone in the Eden process on percolation networks and the ballistic deposition model," *J. Phys. A: Math. Gen.* **18**, L75 (1985).
  - [18] H. K. Janssen, "On Critical Exponents and the Renormalization of the Coupling Constant in Growth Models with Surface Diffusion," *Phys. Rev. Lett.* **78**, 1082 (1997).
  - [19] F. D. A. Aarão Reis, "Numerical study of discrete models in the class of the nonlinear molecular beam epitaxy equation," *Phys. Rev. E* **70**, 031607 (2004).
  - [20] J. M. López, M. Castro, and R. Gallego, "Scaling of Local Slopes, Conservation Laws, and Anomalous Roughening in Surface Growth," *Phys. Rev. Lett.* **94**, 166103 (2005).
  - [21] J. M. López, "Scaling Approach to Calculate Critical Exponents in Anomalous Surface Roughening," *Phys. Rev. Lett.* **83**, 4594 (1999).
  - [22] H. Xia, G. Tang, Z. Xun, and D. Hao, "Numerical evidence for anomalous dynamic scaling in conserved surface growth," *Surf. Sci.* **607**, 138 (2013).
  - [23] F. D. A. Aarão Reis, "Normal dynamic scaling in the class of the nonlinear molecular-beam-epitaxy equation," *Phys. Rev. E* **88**, 022128 (2013).
  - [24] S. Yim and T. S. Jones, "Anomalous scaling behavior and surface roughening in molecular thin-film deposition," *Phys. Rev. B* **73**, 161305 (2006).
  - [25] F. S. Nascimento, S. C. Ferreira, and S. O. Ferreira, "Faceted anomalous scaling in the epitaxial growth of semiconductor films," *EPL (Europhysics Letters)* **94**, 68002 (2011).
  - [26] A. S. Mata, S. C. Ferreira, I. R. B. Ribeiro, and S. O. Ferreira, "Anomalous scaling and super-roughness in the growth of cdtc polycrystalline films," *Phys. Rev. B* **78**, 115305 (2008).
  - [27] J. Krug, "Turbulent interfaces," *Phys. Rev. Lett.* **72**, 2907 (1994).
  - [28] A. Chame and F. Aarão Reis, "Scaling of local interface width of statistical growth models," *Surf. Sci.* **553**, 145 (2004).
  - [29] C. Dasgupta, S. Das Sarma, and J. M. Kim, "Controlled instability and multiscaling in models of epitaxial growth," *Phys. Rev. E* **54**, R4552 (1996).
  - [30] S. Das Sarma, C. J. Lanczycki, R. Kotlyar, and S. V. Ghaisas, "Scale invariance and dynamical correlations in growth models of molecular beam epitaxy," *Phys. Rev. E* **53**, 359 (1996).
  - [31] P. Punyindu and S. Das Sarma, "Noise reduction and universality in limited-mobility models of nonequilibrium growth," *Phys. Rev. E* **57**, R4863 (1998).
  - [32] Z.-p. Xun, Z. Zhang, L. Wu, H. Xia, D.-p. Hao, Y. Yang, Y.-L. Chen, and G. Tang, "Large-scale numerical study on the dynamic scaling behavior of Das Sarma-Tamborenea model by employing noise reduction technique," *EPL (Europhysics Letters)* **111**, 60012 (2015).
  - [33] P. Disrattakit, R. Chanphana, and P. Chatrathorn, "Roughness distribution of multiple hit and long surface diffusion length noise reduced discrete growth models," *Physica A: Stat. Mech. Appl.* **462**, 619 (2016).
  - [34] E. E. M. Luis, T. A. de Assis, and S. C. Ferreira, "Optimal detrended fluctuation analysis as a tool for the de-



- termination of the roughness exponent of the mounded surfaces,” *Phys. Rev. E* **95**, 042801 (2017).
- [35] F. F. Leal, S. C. Ferreira, and S. O. Ferreira, “Modelling of epitaxial film growth with an Ehrlich-Schwoebel barrier dependent on the step height,” *J. Phys. Condens. Matter* **23**, 292201 (2011).
  - [36] F. F. Leal, T. J. Oliveira, and S. C. Ferreira, “Kinetic modelling of epitaxial film growth with up- and downward step barriers,” *J. Stat. Mech. Theory Exp.* **2011**, P09018 (2011).
  - [37] C.-K. Peng, S. V. Buldyrev, S. Havlin, M. Simons, H. E. Stanley, and A. L. Goldberger, “Mosaic organization of DNA nucleotides,” *Phys. Rev. E* **49**, 1685 (1994).
  - [38] W. H. Press, S. A. Teukolsky, W. T. Vetterling, and B. P. Flannery, *Numerical Recipes 3rd Edition: The Art of Scientific Computing*, 3rd ed. (Cambridge University Press, New York, NY, USA, 2007).
  - [39] J. Kertesz and D. E. Wolf, “Noise reduction in Eden models: II. Surface structure and intrinsic width,” *J. Phys. A. Math. Gen.* **21**, 747 (1988).
  - [40] M. Kardar, G. Parisi, and Y.-C. Zhang, “Dynamic Scaling of Growing Interfaces,” *Phys. Rev. Lett.* **56**, 889 (1986).
  - [41] F. Lechenault, G. Pallares, M. George, C. Rountree, E. Bouchaud, and M. Ciccotti, “Effects of Finite Probe Size on Self-Affine Roughness Measurements,” *Phys. Rev. Lett.* **104**, 025502 (2010).
  - [42] S. G. Alves, C. I. L. D. Araujo, and S. C. Ferreira, “Hallmarks of the Kardar-Parisi-Zhang universality class elicited by scanning probe microscopy,” *New J. Phys.* **18**, 093018 (2016).
  - [43] R. Vassoler and G. Zebende, “DCCA cross-correlation coefficient apply in time series of air temperature and air relative humidity,” *Phys. A Stat. Mech. its Appl.* **391**, 2438 (2012).
  - [44] S. G. Alves, T. J. Oliveira, and S. C. Ferreira, “Universality of fluctuations in the Kardar-Parisi-Zhang class in high dimensions and its upper critical dimension,” *Phys. Rev. E* **90**, 020103 (2014).
  - [45] I. S. S. Carrasco and T. J. Oliveira, “Universality and dependence on initial conditions in the class of the non-linear molecular beam epitaxy equation,” *Phys. Rev. E* **94**, 050801 (2016).
  - [46] T. A. de Assis, C. P. de Castro, F. de Brito Mota, C. M. C. de Castilho, and R. F. S. Andrade, “Distribution of scaled height in one-dimensional competitive growth profiles,” *Phys. Rev. E* **86**, 051607 (2012).